Spatio-temporal analysis of the wave front with the GSM

R. Conan*, A. Ziad*, R. Avila*, A. Tokovinin†, F. Martin* and J. Borgnino*

The Date

ABSTRACT

The Generalized Seeing Monitor (GSM) is specifically a monitor of the outer scale. It measures also the seeing angle and the scintillation index. The GSM is operational since one year and its data base contains already the results of three campaign in different astronomical sites. Before the end of the year 1998, two other missions will still extend this data base. These integrated parameters useful for the design of the Adaptive Optics Systems have to be completed by local parameters as the C_n^2 profiles or the wind profiles. With an analysis of the angles of arrival of the wavefront, the GSM is now able to detect the more turbulent layers of the atmosphere and to measure the wind which carries the turbulent eddies inside.

1 Introduction

Since a few years, new telescopes with an aperture of 8–10 meter equipped with Adaptive Optics System (AOS) are building. The astronomical sites where are based these instruments were chosen for their very low seeing angle, for their very low humidity, for the very few numbers of cloudy-days in one year and so one... Among all the atmospheric parameters, there is one for which the effect on the performances of the AOS increases relatively to the size of the aperture of the telescopes : the wave-front outer scale $\mathcal{L}_0$. For example, with a 10 m telescope, the residual error on the wave–front reconstruction after a tip–tilt correction increases as the outer scale decreases[1] and the small $\mathcal{L}_0$ values attenuate the mean square of the low-order Zernike modes.[2] In front of the necessity to obtain a larger knowledge of this parameter, the Generalized Seeing Monitor (GSM) was build. Operational since one year and after three missions in Chile (La Silla), Morocco (Oukaimden) and Uzbekistan (Maydanak), the GSM provides the first data bank on the outer scale. The atmosphere is often described as a pile of turbulent layers. These layers are reduced to one assumed equivalent and the spatial properties of the wave front are well–matched with this single equivalent–layer[3].[4] However, individual informations on the layers can lead to an optimization of the AOS. As shown by Racine,[5] if the altitude of the layers are taken into account and the deformable mirror is conjugated to the altitude of a layer with a high C_n^2, the isoplanatic patch size can double. This is the concept of Altair : the AOS of the Gemini North Canadian telescope. The characteristic time scale of the evolution of the wave front for an AOS gives an estimation of the time that the system can spend in the closed loop. This time depends on the temporal evolution of the layers and is a function of the wind profile.[6] In this paper, after a presentation of the

* Université de Nice–Sophia Antipolis – U.M.R. 6525 Astrophysique, F–06108 Nice Cedex 2, France
† Sternberg Astronomical Institute,Universitetsky prosp., 13, 119899 Moscow, Russia

GSM, a method to determine the wind in a few layers using cross-correlations of the slopes of the wave front is exposed.

2 The presentation of the GSM

2.1 Principle

As explained above, the GSM is a monitor of the outer scale which measures also the seeing angle and the scintillation index. It is constituted of four telescopes with 10 cm apertures (Fig. 1). Each one has a module which measures the angles of arrival (AA) of the wave front incoming from a single unresolved star. The modules are described in Martin et al. (1994).[7] In this standard mode, the GSM measures the atmospheric parameters every four minutes. During the two first minutes, it records the AA and the two other minutes are used for computing. Two telescopes are coupled on the same mount to work as the Differential Image Motion Monitor (DIMM) of the ESO. The four telescopes are disposed in a L–shaped layout (Fig. 2) to allow the measurements of the speed and the direction of the winds. This configuration permits to construct six baselines for the cross-analysis between the AA. The comparison between the six experimental spatial-covariances of the AA and a grid of theoretical one leads to six values of $\mathcal{L}_0$. The final value is the median of the six. The theoretical spatial-covariances are computed from the Von Kàrmàn power–spectrum of the phase. The seeing angle ε is deduced from the variance of the AA measured individually with each telescope and differentially with the two telescopes coupled. As the GSM measures also the flux of the star, the dispersion of the flux, corrected from noise, provides the scintillation index σ_I^2.

Figure 1 : The GSM instrument at La Silla

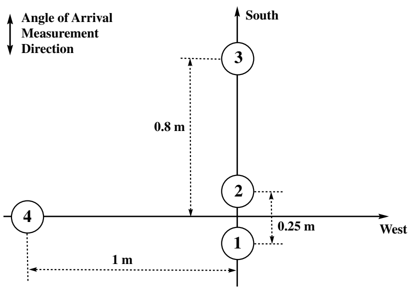

Figure 2 : The layout of the GSM

.

2.2 Results obtained for $\mathcal{L}_0$, ε and σ_I^2 at La Silla (Chile) and at Maydanak (Uzbekistan)

The figures 3 and 4 present these three parameters measured respectively at La Silla (Chile) in August–September of 1997 and at Maydanak (Uzbekistan) in July of 1998. The two graphs show the parameters versus the time over the whole mission and the corresponding histograms. For both missions, a DIMM worked near the GSM and a good agreement was found between the seeing measured by both instruments.

2.2.1 La Silla

The mission ran for 14 nights. The mean value of $\mathcal{L}_0$, ε and σ_I^2 are respectively 25 m, 1.7 arcsec and 4.4%. The mean value of ε is strongly higher than the typical values registered at La Silla. The statistical distributions of $\mathcal{L}_0$ and σ_I^2 look like a log–normal distribution as the distribution of ε is not. The seeing ε is more dependent of the C_n^2 in the surface layer than the two other parameters. σ_I^2 depends principally on the C_n^2 of the layers in the free atmosphere and $\mathcal{L}_0$ is the mean weighted by the C_n^2 of the geophysical outer scale. So the difference between the distributions of $\mathcal{L}_0$ and σ_I^2 on the one hand and the distribution of ε on the other hand could revealed an active surface layer at La Silla during this period. It could also explained the high values of ε.

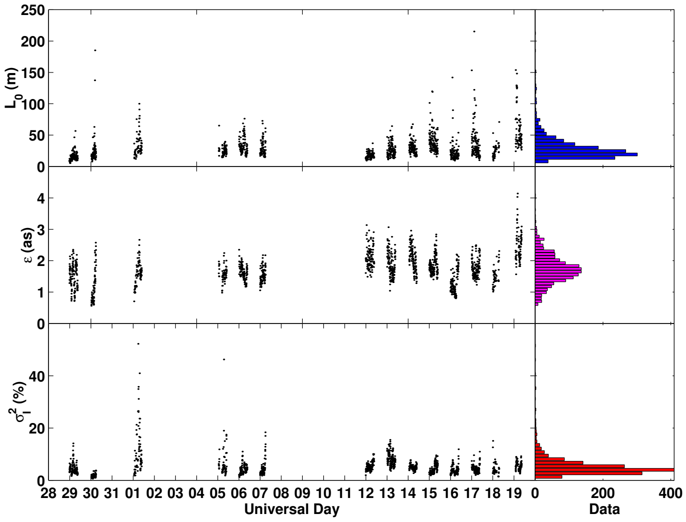

Figure 3 : La Silla (Chile) August 28 – September 19 1997

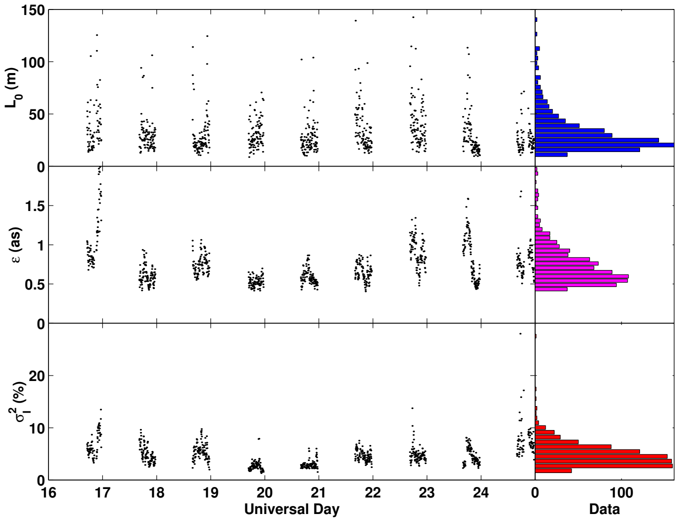

Figure 4 : Maydanak (Uzbekistan) July 16–24 1998

2.2.2 Maydanak

The mission ran for 9 nights. The mean value of $\mathcal{L}_0$, ε and σ_I^2 are respectively 32 m, 0.7 arcsec and 4.4%. The distributions of the three parameters are quasi log–normal. The mission at Maydanak are remarkable for the stable meteorological conditions and for the very low seeing angles.

3 Analysis of the spatio-temporal cross-correlation of the AA

3.1 Principle

The objective here is to measure the wind in the layers which deteriorate the wave front. The following demonstration is based on two assumptions. The first one is that the whole atmosphere is a pile of turbulent layers and the second is that the Taylor hypothesis is true in each layer. The first hypothesis is now well–verified by the C_n^2 profiles measured since many years and the evidence of the second will be made by the comparison with the winds measured by the weather station of the DIMM. On the figure 5, two of the six baselines and the wind direction of a layer are drawn on the schematic layout of the GSM. From this graph, an important time can be defined : the time $\Delta\tau_{ij}$ taken by a turbulent eddy, carried by the wind, to be detected successively by two telescopes. This time depends on the baseline which links up the two telescopes and on the wind[8] as follows :

$$\Delta\tau_{ij} = \frac{B_{ij}\cos(\gamma_{ij}-\eta)}{v},$$

where i and j represent the telescopes and the couple (B_{ij},γ_{ij}) and (v,η) are the polar coordinates of the baseline vector and of the wind vector respectively. In the cross-correlation between the AA measured by the telescopes i and j, $\Delta\tau_{ij}$ corresponds also to the position of the peak due to the motion of the eddy of the layer characterized by the wind (v,η). The aim being to find both speed v and direction η of the wind, another baseline, non parallel to the first one, gives another $\Delta\tau_{kl}$ and the two equations lead to the polar coordinates of the wind vector. In fact, with the six baselines, 15 couples of equations exist and the elimination of the couples of baselines parallel (1.2, 2.3, 1.3) or nearly parallel (1.4, 2.4) gives finally 11 couples of equations. The final wind is the mean of the 11 winds.

The figure 6 is an example of the six cross-correlations. The units are the corresponding telescopes. It is a zoom between −1 and +1 second of the complete cross-correlations which vary from −2 mn to +2 mn. The positions of the peaks give a wind which blows approximately from the north at 25 m/s.

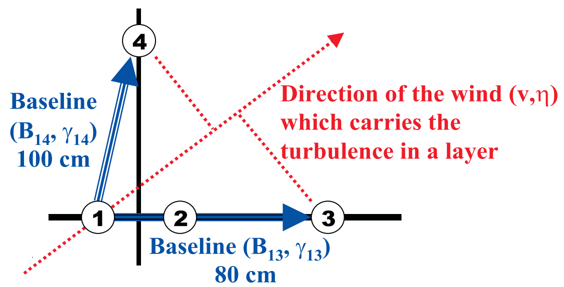

Figure 5 : Baselines and wind

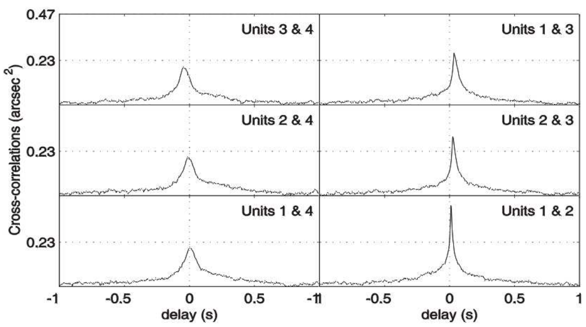

Figure 6 : La Silla 18 Sept. 1998 – 02:53 UT

4 Temporal evolution of the cross-correlations of the AA

4.1 Snapshots at La Silla and at Maydanak

In the precedent example (fig. 6), one layer is put in evidence but most of the time, until 4 layers are detected and the winds measured. The cross–correlation shape becomes a multi–peak cross–correlation associated with the multi–layer structure of the atmosphere. Keeping in mind that a peak is related to a layer and that the GSM records the AA every four minutes, the trace of the layers is followed all the night long. Both following sets of graphs for the La Silla and Maydanak missions represent a few extracts of the total sets of cross-correlation of two nights. Each graph shows the cross-correlations as defined in the figure 6 and the corresponding values of the Fried parameter r_0, the outer scale $\mathcal{L}_0$ and the scintillation σ_I^2. The speed and the direction of the wind are deduced from the position of the highest peak of the cross–correlation. The cross indicates the current value and the dots the past values. The graphs are plotted chronologically and must be read from the left to the right and from the top to the bottom.

- Cross-correlations of the AA at La Silla (September 15 1997) (Figure 7)

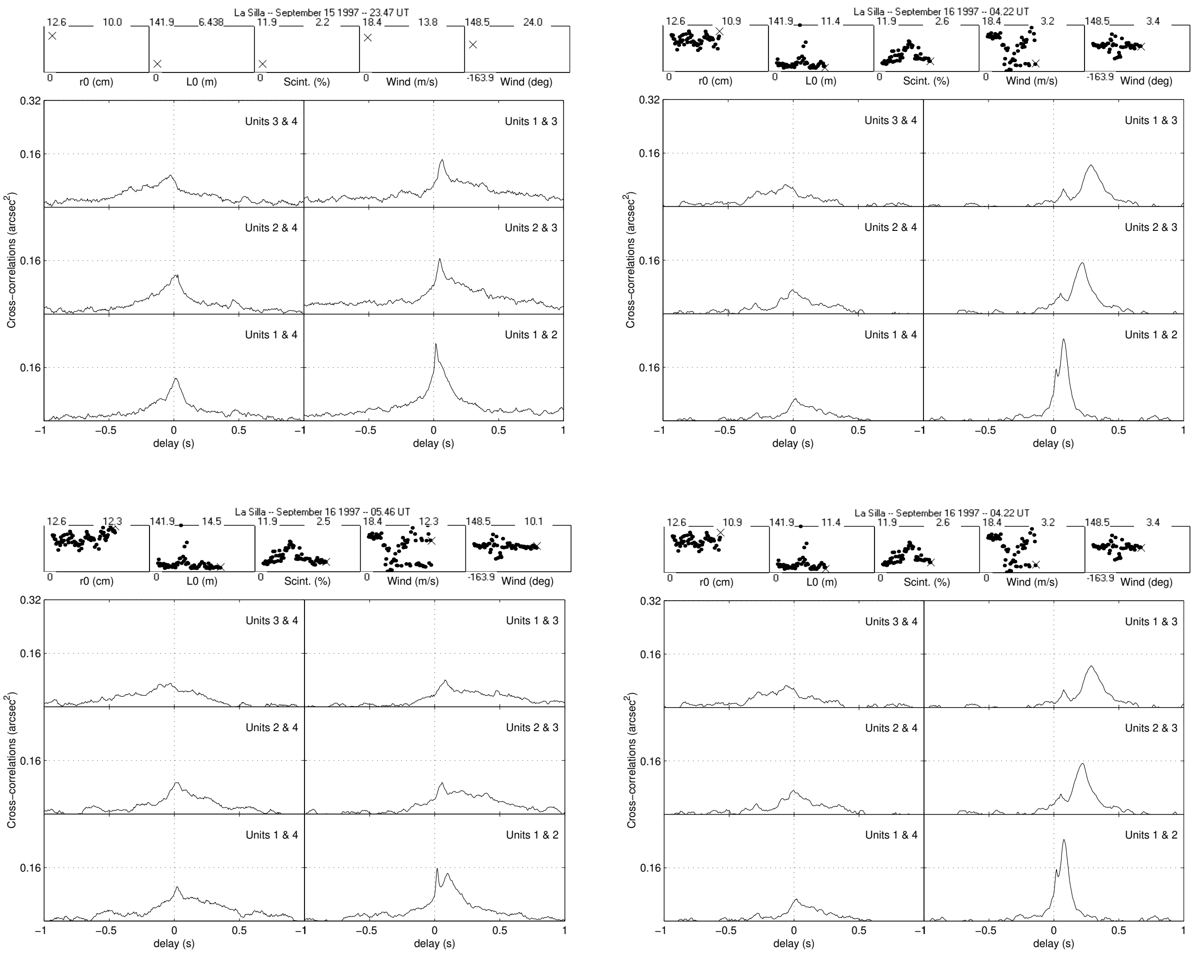

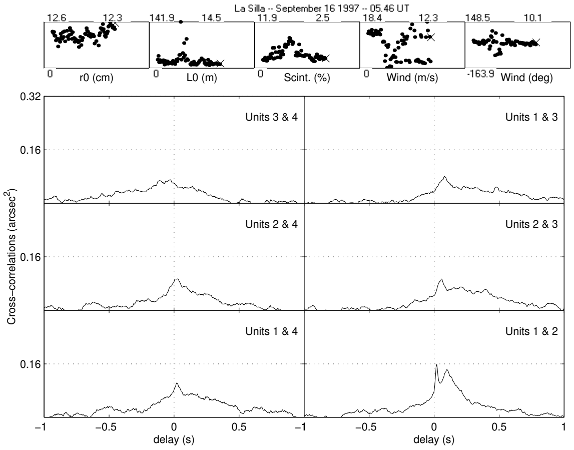
La Silla -- September 16 1997 -- 05.46 UT
12.6 12.3 141.9 14.5 11.9 2.5 18.4 12.3 148.5 10.1
0 r0 (cm) 0 L0 (m) 0 Scint. (%) 0 Wind (m/s) -163.9 Wind (deg)
Units 3 & 4
Units 1 & 3
Units 2 & 4
Units 2 & 3
Units 1 & 4
Units 1 & 2
Cross-correlations ($arcsec^2$)
delay (s)

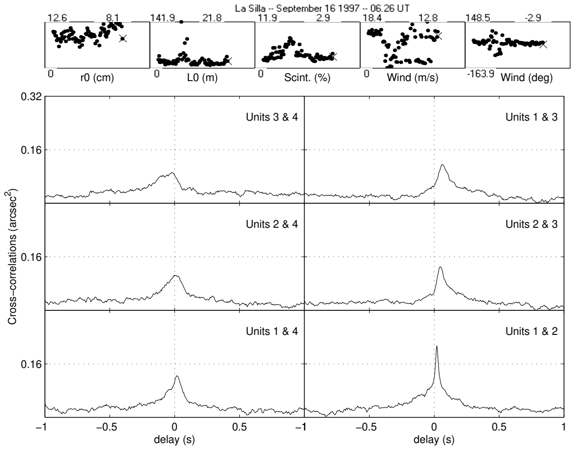
La Silla -- September 16 1997 -- 06.26 UT
12.6 8.1 141.9 21.8 11.9 2.9 18.4 12.8 148.5 -2.9
0 r0 (cm) 0 L0 (m) 0 Scint. (%) 0 Wind (m/s) -163.9 Wind (deg)
Units 3 & 4
Units 1 & 3
Units 2 & 4
Units 2 & 3
Units 1 & 4
Units 1 & 2
Cross-correlations ($arcsec^2$)
delay (s)

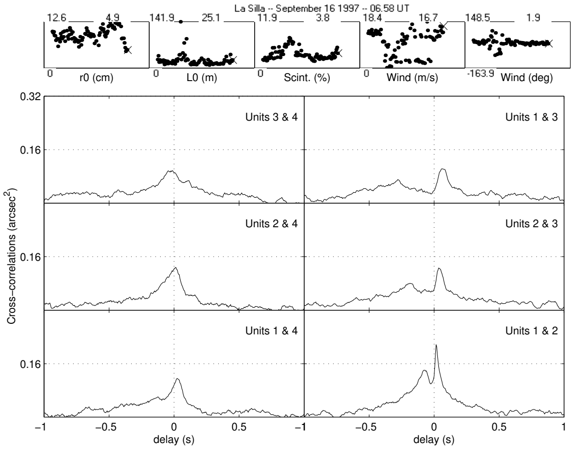
La Silla -- September 16 1997 -- 06.58 UT
12.6 4.9 141.9 25.1 11.9 3.8 18.4 16.7 148.5 1.9
0 r0 (cm) 0 L0 (m) 0 Scint. (%) 0 Wind (m/s) -163.9 Wind (deg)
Units 3 & 4
Units 1 & 3
Units 2 & 4
Units 2 & 3
Units 1 & 4
Units 1 & 2
Cross-correlations ($arcsec^2$)
delay (s)

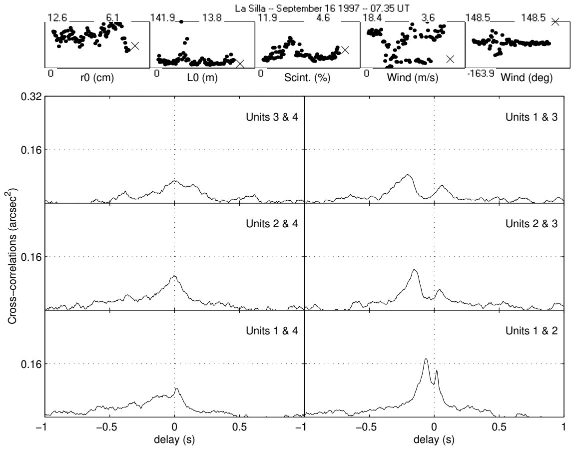
La Silla -- September 16 1997 -- 07.35 UT
12.6 6.1 141.9 13.8 11.9 4.6 18.4 3.6 148.5 148.5
0 r0 (cm) 0 L0 (m) 0 Scint. (%) 0 Wind (m/s) -163.9 Wind (deg)
Units 3 & 4
Units 1 & 3
Units 2 & 4
Units 2 & 3
Units 1 & 4
Units 1 & 2
Cross-correlations ($arcsec^2$)
delay (s)

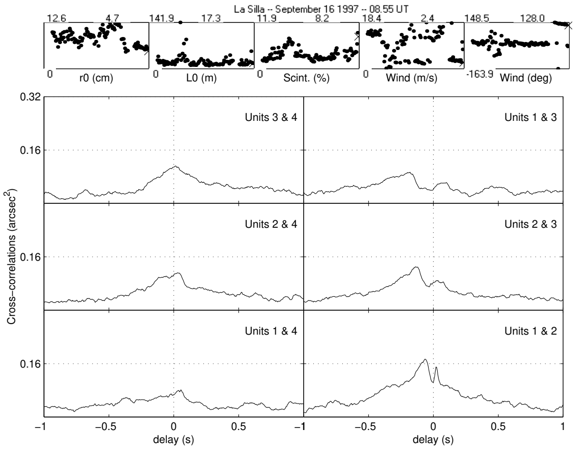
La Silla -- September 16 1997 -- 08.55 UT
12.6 4.7 141.9 17.3 11.9 8.2 18.4 2.4 148.5 128.0
0 r0 (cm) 0 L0 (m) 0 Scint. (%) 0 Wind (m/s) -163.9 Wind (deg)
Units 3 & 4
Units 1 & 3
Units 2 & 4
Units 2 & 3
Units 1 & 4
Units 1 & 2
Cross-correlations ($arcsec^2$)
delay (s)

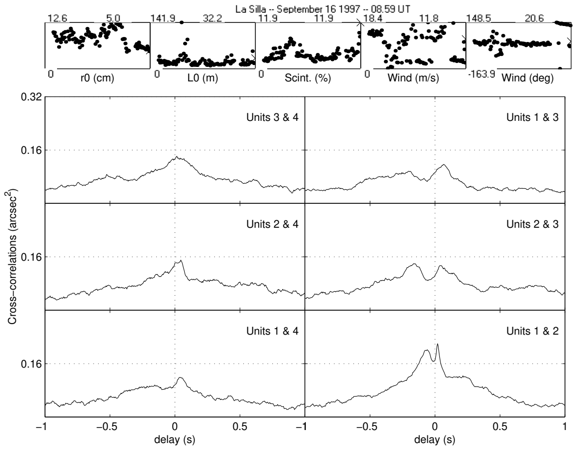
La Silla -- September 16 1997 -- 08.59 UT
12.6 5.0 141.9 32.2 11.9 11.9 18.4 11.8 148.5 20.6
0 r0 (cm) 0 L0 (m) 0 Scint. (%) 0 Wind (m/s) -163.9 Wind (deg)
Units 3 & 4
Units 1 & 3
Units 2 & 4
Units 2 & 3
Units 1 & 4
Units 1 & 2
Cross-correlations ($arcsec^2$)
delay (s)

- Cross-correlations of the AA at Maydanak (July 23 1998) (Figure 8)

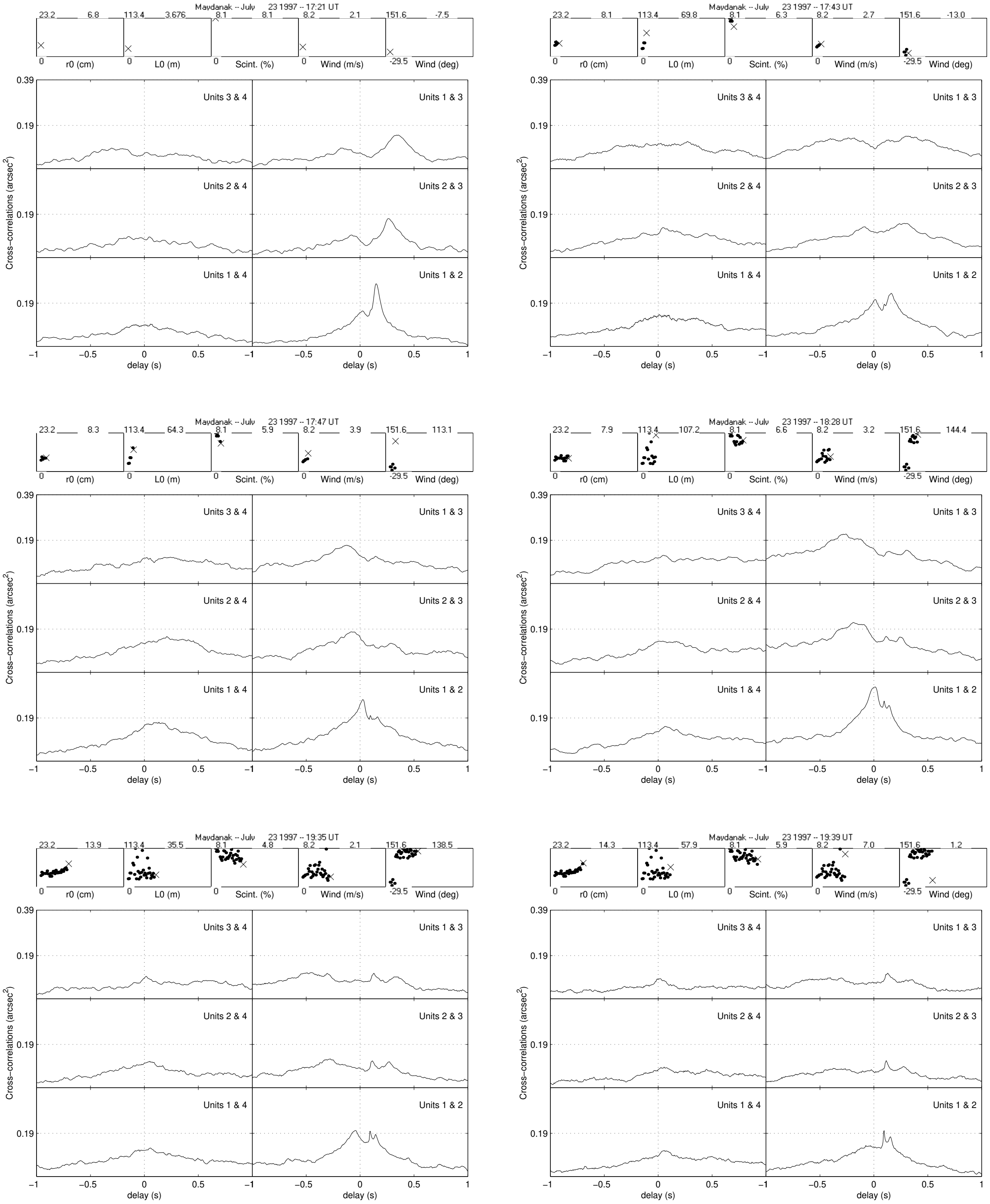

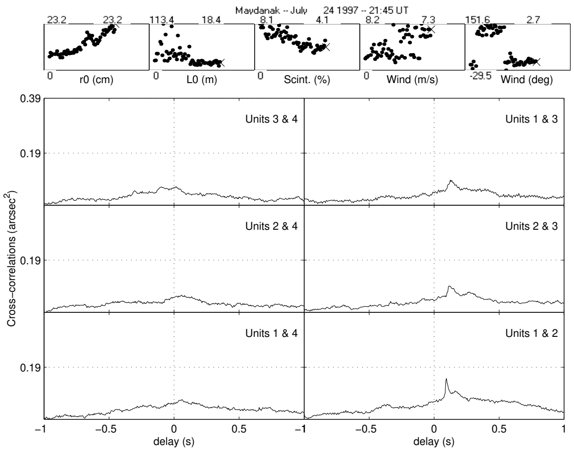

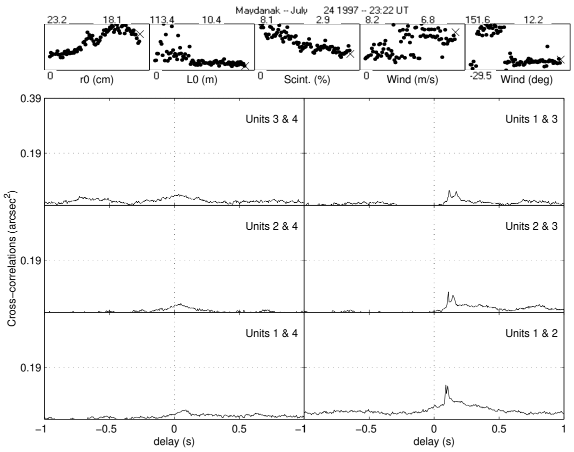

4.2 Discussion

The speed and the direction of the winds measured during both nights at La Silla and at Maydanak are reported on the polar graphs, figures 9 and 10 respectively.

On the figure 9, the asterisks represent the winds related to the peak called "closer peak" which is the peak detected all the night and always the nearest of the zero delay line. The other winds are plotted with dots and the diamonds show the winds measured by the weather station of the DIMM. The analysis of the cross–correlations bring out three different winds and let supposed three layers. But the comparison between the winds of the GSM and the winds of the weather station demonstrates the existence of only two layers because for one of them the direction of the wind has changed. And a variation in the direction of the wind causes a variation in the position $\Delta\tau_{ij}$ of the associated peak. The night of September 15 is typical of the winds measured at La Silla during this period. Almost each night, two layers were detected. One gives winds which match the winds measured by the weather station and the other layer have winds blowing all nights in the same direction. The fact that the Taylor hypothesis permits to deduce wind characteristics which are confirmed by another independent measurement proves its validity. The altitude of the layers remains unknown but for the layer which have the same wind than that one measured by the weather station, it is obvious that it is the surface layer.

For Maydanak, the cross–correlations put in evidence four layers well–identified because, during the night, all the combinations of pairs or triplets of layers appear successively. Three winds blow approximately in the direction of the east but with three different speeds : lower than 4m/s, higher than 6.8m/s and between both. The last wind blows in the north–west direction at a speed inferior at 5m/s.

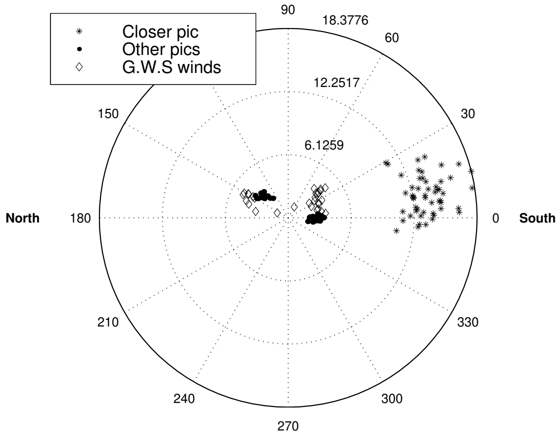

Figure 9 : Winds measured at La Silla

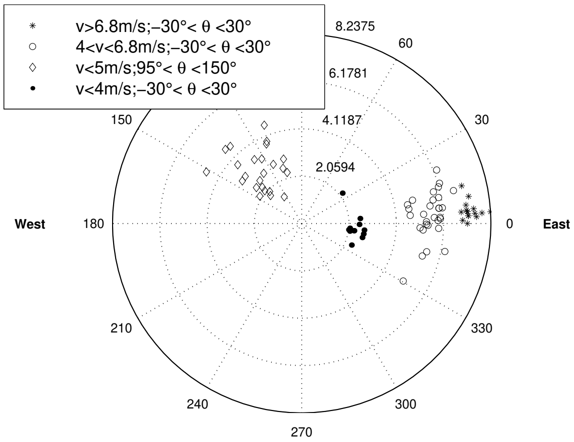

Figure 10 : Winds measured at Maydanak

5 Conclusion

The GSM is an instrument which has evolved since its first mission at La Silla (Chile). At first, it gave just the outer scale, the seeing and the scintillation. The analysis of the cross–correlation of the AA has shown how the GSM detects also the predominant turbulent layers and how it measures their winds. The new improvement is the measurement of the isoplanatic angle. The mission at Maydanak was also used to compare the isoplanatic angle measured by the GSM and by the isoplanometer of the team of the Sternberg Astronomical Institute of the University of Moscow ([1]http://www–astro.unice.fr/GSM/Publications/Maydanak_report.ps). A very good agreement was found between both series of data. Now, the GSM is the unique portable instrument able to provide a so complete set of atmospheric parameters for the optical astronomy. The name of the instrument has followed the evolution, the acronym GSM remains but at the beginning it means Grating Scale Monitor due to the conception of the modules which measure the AA and to the main purpose fixed to the experiment.

[1]A Web server for the GSM data is under construction in order that the scientific community can consult the growing data base of the GSM and particularly the unique data base concerning the outer scale (URL : http://www–astro.unice.fr/GSM).

Henceforth the Generalized Seeing Monitor denomination is more adapted to its widened competencies. Two other missions have occurred at Oukaimden in Morocco and at Maydanak in Uzbekistan. In October 1998, a new mission will take place at the Cerro Pachon in Chile, the site of the Gemini South telescope. The GSM will work simultaneously with the Generalized Scidar of the Department of Astrophysic of the University of Nice[9] and in–situ profiles of pressure, temperature, humidity, C_n^2 and wind will be collected with sounding–balloons. It will be the first time than these different instruments dedicated to the study of the atmosphere are gathered on the same site and the expected result is a better understanding of the effects of the turbulent phenomena in optical astronomy. The last mission of the year 1998 will be at Cerro Paranal in December.

6 REFERENCES

[1] V.V. Voitsekhovich and S. Cuevas. Adaptive optics and the outer scale of turbulence. *J. Opt. Soc. Am. A*, 12(11):2523–2531, 1995.

[2] D.M. Winker. Effect of a finite outer scale on the zernike decomposition of atmospheric optical turbulence. *J. Opt. Soc. Am.*, 8(10):1568–1573, October 1991.

[3] V.I. Tatarskii. *The effects of the turbulent atmosphere on wave propagation*. Israel Program for Scientific Translations, Jerusalem, 1971.

[4] F. Roddier. The effect of atmospheric turbulence in optical astronomy. In *Progress in Optics*, volume XIX. E. Wolf, 1981.

[5] R. Racine and B.L. Ellerbroek. Profiles of night–time turbulence above mauna–kea and isoplanatism extension in adaptive optics. *Proc. SPIE*, 2534:248–257, 1995.

[6] F. Roddier, J.M. Gilli, and G. Lund. On the origin of speckle boiling and its effects in stellar speckle interferometry. *J. Optics (Paris)*, 13(5):263–271, 1982.

[7] F. Martin, A. Tokovinin, A. Agabi, J. Borgnino, and A. Ziad. G.s.m. : a grating scale monitor for atmospheric turbulence measurements. i. the instrument and first results of angle of arrival measurements. *Astron. Astrophys. Suppl. Ser.*, 108:173–180, 1994.

[8] R. Avila, A. Ziad, J. Borgnino, F. Martin, A. Agabi, and A. Tokovinin. Theoretical spatio-temporal analysis of angle of arrival induced by atmospheric turbulence as observed with the grating scale monitor experiment. *J. Opt. Soc. Am. A*, 14(11):3070–3082, November 1997.

[9] R. Avila, J. Vernin, , and E. Masciadri. Whole atmospheric-turbulence profiling with generalized scidar. *Applied Optics*, 36(30):7898–7905, October 1997.